THE ASTROPHYSICAL JOURNAL, 473:356–364, 1996 December 10


# THE TYPE Ia SUPERNOVA RATE AT $z \sim 0.4$

R. PAIN,[1,2] I. M. HOOK,[1,3] S. DEUSTUA,[1] S. GABI,[1] G. GOLDHABER,[1,4] D. GROOM,[1] A. G. KIM,[1]
M. Y. KIM,[1] J. C. LEE,[1] C. R. PENNYPACKER,[1,5] S. PERLMUTTER,[1,4] I. A. SMALL,[1] A. GOOBAR,[6]
R. S. ELLIS,[7] R. G. MCMAHON,[7] K. GLAZEBROOK,[8] B. J. BOYLE,[9] P. S. BUNCLARK,[9]
D. CARTER,[9] AND M. J. IRWIN[9]
(THE SUPERNOVA COSMOLOGY PROJECT)
*Received 1996 March 27; accepted 1996 June 28*

## ABSTRACT

We present the first measurement of the rate of Type Ia supernovae at high redshift. The result is derived by using a large subset of data from the Supernova Cosmology Project. Three supernovae were discovered in a surveyed area of 1.7 deg$^2$. The survey spanned a $\sim 3$ week baseline and used images with 3 $\sigma$ limiting magnitudes of $R \sim 23$. We present our methods for estimating the numbers of galaxies and the number of solar luminosities to which the survey is sensitive, as well as the supernova detection efficiency, which is used to determine the control time, the effective time for which the survey is sensitive to a Type Ia event. We derive a rest-frame Type Ia supernova (SN) rate at $z \sim 0.4$ of $0.82^{+0.54+0.37}_{-0.37-0.25}\ h^2$ SNu (1 SNu = 1 SN per century per $10^{10} L_{B\odot}$), where the first uncertainty is statistical and the second includes systematic effects. For the purposes of observers, we also determine the rate of SNe, per sky area surveyed, to be $34.4^{+23.9}_{-16.2}$ SNe yr$^{-1}$ deg$^{-2}$ for SN magnitudes in the range $21.3 < R < 22.3$.

*Subject headings:* stars: statistics — supernovae: general — surveys

## 1. INTRODUCTION

Type Ia supernovae (SNe) may provide one of the best testable distance indicators at high redshifts, where few reliable distance indicators are available with which to study the cosmological parameters. A direct measurement of SN rates is therefore important in developing systematic programs to find and study such high-redshift Type Ia SN distance indicators. Supernova rates at high redshift are also important for understanding galaxy evolution, star formation rates, and nucleosynthesis rates. The dependence of the Type Ia SN rate on redshift can be used to constrain models for the progenitors of the SN explosion. For example, Ruiz-Lapuente, Burket, & Canal (1995) have discussed the correlation of Type Ia SN rate and explosion time with parent population age and galaxy redshift.

Beginning with the discovery of SN 1992bi (Perlmutter et al. 1995b), we have developed search techniques and rapid analysis methods that allow systematic discovery and follow up of "batches" of high-redshift supernovae. At the time of this analysis, the search had discovered seven SNe at redshifts $z = 0.3$–$0.5$ (Perlmutter et al. 1994, 1995b, 1995c). We report here our first estimates of the SN Ia rate at high $z$ based on a subset of this data set. We are currently following a further 11 SNs in the range $0.15 < z < 0.65$ (Perlmutter et al. 1995a), but the data collection and the analysis of these SNe are not yet complete.

The observing strategy developed for our search compares large numbers of galaxies in each of $\sim 50$ fields observed twice with a separation of $\sim 3$ weeks; thus almost all our SNe are discovered before maximum light. This search schedule makes it possible to precisely calculate the "control time," the effective time during which the survey is sensitive to a Type Ia event. On the other hand, since hundreds of anonymous high-redshift galaxies are observed in each image, it is more difficult than for nearby SN searches to estimate the number, morphological type, and luminosities of galaxies searched in a given redshift range.

The method used to calculate the rate can be divided into two main parts: (1) estimation of the SN detection efficiency, and hence the control time, and (2) estimation of the number of galaxies and the total stellar luminosity (measured in $10^{10} L_{B\odot}$) to which the survey is sensitive. We have studied our detection efficiency as a function of magnitude and supernova–to–host galaxy surface brightness ratio by using Monte Carlo techniques. By comparing galaxy counts per apparent-magnitude interval in our images to the study of Lilly et al. (1995), we have estimated the number of galaxies in a given interval of redshift and apparent magnitude. The galaxy counts and efficiency studies, together with the number of confirmed SN detections in this set of images, yield an estimate of the SN Ia rate at $z \sim 0.4$.

In § 2 of this paper, we describe the data that we have used. Section 3 deals with the determination of the efficiency of the search and, hence, the control times. Section 4 covers the method for estimating galaxy counts. In § 5, we derive the Type Ia rate at $z \sim 0.4$; in § 6, we estimate the systematic uncertainty; and in § 7, we discuss the results.

## 2. DATA SET

For this analysis, we studied a set of 52 similar search fields observed in 1993 December and 1994 January. This is the first sizable data set to arise from the Supernova Cosmology Project. These images are suitable for a determi-

[1] Lawrence Berkeley National Laboratory, Berkeley, CA 94720.
[2] Laboratoire de Physique Nucléaire et de Hautes Energies, Centre National de la Recherche Scientifique–IN2P3, and Universités Paris VI and VII, France.
[3] Department of Astronomy, University of California, Berkeley, Berkeley, CA 94720.
[4] Center for Particle Astrophysics, University of California, Berkeley, Berkeley, CA 94720.
[5] Space Sciences Laboratory, University of California, Berkeley, Berkeley, CA 94720.
[6] Universitet Stockholms, S-106 91 Stockholm, Sweden.
[7] Institute of Astronomy, University of Cambridge, Madingley Road, Cambridge CB3 0HA, England.
[8] Anglo-Australian Observatory, P.O. Box 296, Epping, NSW 2121, Australia.
[9] Royal Greenwich Observatory, Madingley Road, Cambridge CB3 0EZ, England.

nation of the SN rate since they were obtained under similar conditions with a single camera at one telescope and therefore form a well-defined, homogeneous set.

The data were obtained by using the "thick" 1242 × 1152 EEV5 camera at the 2.5 m Isaac Newton Telescope, La Palma. The projected pixel size is 0.″56, yielding an image area of approximately 11′ × 11′. Exposure times were 600 s in the Mould $R$ filter, and the individual images typically reach a 3 $\sigma$ limit of at least $R \sim 23$ mag. Seeing was typically $\sim$1.″4. The fields lie in the range $2^h < \alpha(\mathrm{B1950}) < 14^h$ and $\delta(\mathrm{B1950}) > -10°$, excluding the Galactic plane ($|b| \gtrsim 30°$). Many of the fields were selected because of the presence of a high-redshift cluster ($z \sim 0.4$). Suitable clusters and their redshifts were taken from Gunn, Hoessel, & Oke (1986). The effect of the presence of clusters in the survey fields is taken into account in the calculation of the SN rate (see § 4).

For most fields, two first-look "reference" images were obtained, here called $\mathrm{ref}_1$ and $\mathrm{ref}_2$, and for all fields two second-look "search" images ($\mathrm{search}_1$, $\mathrm{search}_2$) were obtained 2–3 weeks after the reference images. The useful area of this data set is defined by the overlap area of the original set of reference images with the second set of search images. The total useful area covered in this study is 1.73 $\mathrm{deg}^2$.

The analysis procedure and method for finding SNe can be summarized as follows: The images were flat-fielded, and zero points for the images were estimated by comparison with $E$ (red) magnitudes of stars in the APM (Automated Plate Measuring Facility, Cambridge, England) POSS I catalog (McMahon & Irwin 1992).

For the final analysis of the SN light curves for the determination of $q_0$, the fields containing SNe are reobserved and calibrated by using Landolt standards (Landolt 1992). However, this calibration is not available for all our search fields that do not contain SNe, hence the use of APM calibration for this study. A comparison of APM $E$ magnitudes with CCD $R$ magnitudes shows that $E-R$ has a mean of $-0.2$ mag and rms 0.2 mag. We therefore applied a 0.2 mag shift to the APM magnitudes. The uncertainty in the rate introduced by the uncertainty in the zero points is discussed in § 6.

The search images were combined (after convolution to match the seeing of the worst of the four images), and the combined reference images were subtracted from this after scaling in intensity. The resulting difference image for each field was searched for SN candidates. The main selection criteria was that the object must be a 4 $\sigma$ detection on the difference image. The candidate list was filtered by requiring that the object not move by more than 2 pixels between the two search images (to remove asteroids) and that the object be a 2.5 $\sigma$ detection on the separate difference images [i.e., $\mathrm{search}_1 - (\mathrm{ref}_1 + \mathrm{ref}_2)$ and $\mathrm{search}_2 - (\mathrm{ref}_1 + \mathrm{ref}_2)$]. There was no requirement that the candidate be on a visible host galaxy. The remaining candidate SNe on all the images were inspected visually for obvious problems, such as very bright stars nearby or bad columns, that could affect the photometry. Follow-up photometry and spectroscopy were used to determine the SN types.

In this subset of the search data three SNe were found, with redshifts 0.374, 0.420, and 0.354. Their properties are summarized in Table 1. SN 1994H was discovered in a field centered on a cluster (Abell 370). Its host galaxy is at the cluster's redshift ($z_{\mathrm{clus}} = 0.373$) at a projected distance of 1.′1.

TABLE 1

SUMMARY OF THE THREE SUPERNOVAE

| Name | $z$ | Host $R$ Magnitude | Distance from Host Core (arcsec) | Discovery $R$ Magnitude |
|---|---|---|---|---|
| 1994H..... | 0.374 | 21.1 | 1.0 | 21.6 |
| 1994al..... | 0.420 | 21.2 | 1.0 | 22.6 |
| 1994F ..... | 0.354 | 20.2 | 2.8 | 22.5 |

The redshifts were determined from spectra of the host galaxies. For the purposes of this analysis, we assume that these are all Type Ia SNe. This is a likely scenario since Type Ia's are the brightest of the SN types and, therefore, the most likely to be detected at large distances. The measured light curves of the three SNe follow the standard Type Ia light-curve template (Leibundgut 1988). The data, however, could be consistent with unusually bright Type II-L supernovae. Using our previous estimate of one very bright Type II-L SN per 10 Type Ia SNe (Perlmutter et al. 1995b), we expect at most 0.3 Type II-L SNe in the sample. This in agreement with our recent discovery of 11 supernovae among which 10 are consistent with being Type Ia SNe and one with being a Type II (Perlmutter et al. 1995a). For SN 1994F, we also have a spectrum, and it is consistent with that of a Type Ia SN at the date of observation. Other spectra that we have obtained for the larger sample of SNe discovered in 1994 are also consistent with those of Type Ia SNe. In addition, in this larger sample, one of the SNe for which no spectrum was obtained was in an elliptical host galaxy, a strong indicator of Type Ia identification. A full discussion of the light curves and spectra will be given in a future paper (Perlmutter et al. 1996b).

During reanalysis of the data for the purposes of calculating the rate, another faint ($R = 22.5$) object was found. This candidate SN, which was very near the detection threshold, had not been classified as an SN at the scanning stage (final visual inspection) during the first analysis. It had therefore not been followed but cannot be ruled out as a possible supernova. The object shows a fairly large motion between the two search images (0.″5, or $\sim$1 pixel), which indicates that it may be a faint asteroid. Although unlikely, the possibility that the object is a Type Ia SN was taken into account in the systematic uncertainty, as discussed in § 6.

## 3. CONTROL TIMES AND DETECTION EFFICIENCIES

A naive estimate of the control time, $\Delta T$, is given by the time during which the supernova light curve is above a given threshold corresponding to the limiting magnitude of the observations. In our case this significantly overestimates the control time, for the following reasons.

The data presented here were obtained with an observing strategy designed to measure $q_0$ by conducting a search for SNe on the rise (before their maximum light) using a subtraction technique. The signal on the search image must therefore be significantly larger than that on the reference image, reducing $\Delta T$ from the naive estimate by approximately a factor of 2. In addition, the detection efficiency depends on the host galaxy's magnitude, the image quality, the search technique, and strongly on the magnitude of the supernova at the detection time.

In this analysis, we compute a control time equal to the weighted sum of days during which the SN can be detected,

where the weighting is by the corresponding detection efficiency, $\epsilon$. The control time is given by $\Delta T = \int \epsilon(t)dt$, where $\epsilon$ is a function of the observed magnitude $m_{obs}$, which is itself a function of time $t$ relative to maximum, and $\delta t$, the time separation of the search and reference images. To account for the $z$-distribution of galaxies in the fields, control times were calculated in bins of $z$ (and host galaxy magnitude). We assumed that SN magnitude as a function of time follows the average of the best-fit, time-dilated and $K$-corrected Leibundgut Type Ia template light curves. The generalized $K$-correction described by Kim, Goobar, & Perlmutter (1996) was used here.

The three light curves that we use as example high-redshift SNe were calibrated by using Landolt standards (Landolt 1992). Since these are observed light curves, in *apparent* magnitude, no explicit dependence of our rate result on $H_0$ or $q_0$ is introduced at this stage. The control time was computed by taking Galactic extinction into account separately for each field. The reddening values for each field, $E(B-V)$, were supplied by D. Burstein (1995, private communication, derived from the analysis of Burstein & Heiles 1982) and were applied to the data by assuming $R_V = 3.1$ and $A_R/A_V = 0.751$ (Cardelli, Clayton, & Mathis 1989).

The detection efficiency $\epsilon$ is a complicated function of many parameters. The efficiency as a function of SN magnitude depends on the quality of the subtracted images (seeing, transmission) together with the detailed technique (convolution, selection criteria) used to extract the "signal" (SN candidates) from the "background" (e.g., cosmic rays, asteroids, bad subtractions). In addition, there is a slight dependence on the host galaxy magnitude. The detection efficiency was calculated by using a Monte Carlo method. A synthetic image was created for every field by adding simulated supernovae to the search images. The reference images were subtracted from the synthetic search images using exactly the same software as used for the supernova search, described in § 2, and the number of simulated SNe that satisfied the selection criteria was determined. This technique allows us to measure detection efficiencies as a function of supernova magnitude individually for every field, thus taking into account the other parameters mentioned above. The efficiency derived in this way includes the effects of parts of the image being unusable for the SN search, e.g., as a result of bright foreground stars.

One hundred simulated SNe were placed on each search image, with a range of SN apparent magnitude, host galaxy apparent magnitude, and locations with respect to host galaxies. Each simulated SN was generated by scaling down and shifting a bright star from that image, with signal-to-noise ratio greater than 50, from the image being studied. The position relative to the host galaxy was chosen at random from a normal distribution with 1 $\sigma$ equal to the half-width at half-maximum of the galaxy. The shift of the scaled bright star to the host galaxy was by an integral number of pixels, to maintain the pixelized point-spread function. Since noise fluctuations in the sky background strongly dominate the SN photon noise, it was not necessary to add extra Poisson noise to these simulated SNe.

Figures 1*a*–1*c* show the fractional number of simulated SNe recovered as a function of SN magnitude (at detection) for the three fields in which SNe were found. Figure 1*d* shows the efficiency as a function of relative surface brightnesses of the SN and host galaxy. This last parameter gives

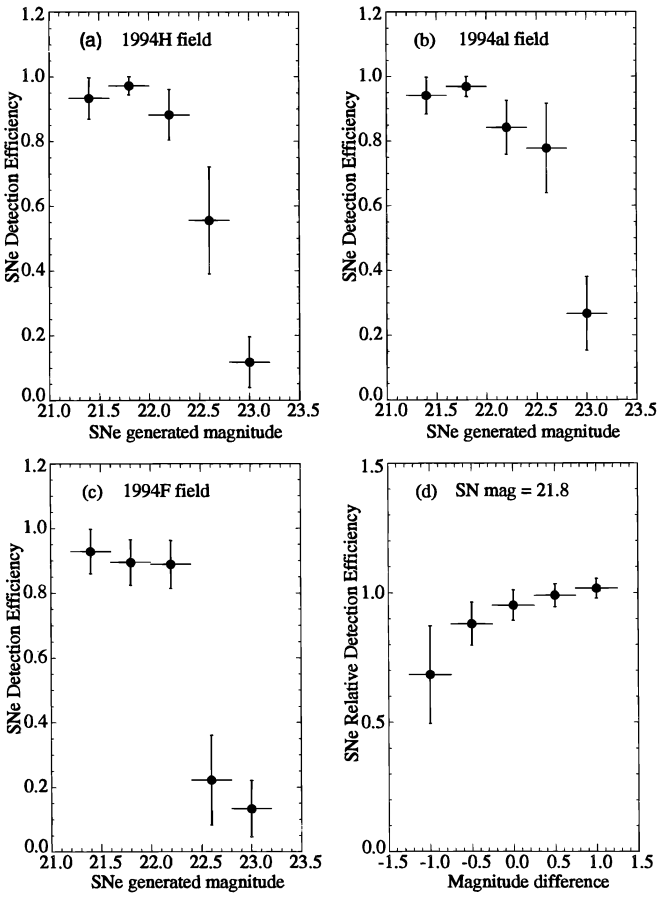


FIG. 1.—(*a*–*c*) Detection efficiency as a function of magnitude for the three difference images in which SNe were found. The vertical error bars show the 1 $\sigma$ statistical uncertainty, and the horizontal bars show the bin ranges. (*d*) Detection efficiency as a function of relative SN-to-host surface brightness.

an indication of the effect of SN location with respect to the host galaxy. Although this is a small effect, it was taken into account. For a typical field, the detection efficiency is over 85% for any added fake stellar object brighter than $R = 22.0$ (note that the more recent searches of this project have worked with significantly deeper images).

At this stage, we are able to determine the "survey rate" of SN discoveries that a search for Type Ia SNe can expect to obtain per square degree. We give the rate in a range of 1 mag in $R$, centered on the mean peak $R$ magnitude of the three SNe found in this search, $R = 21.8$. The survey rate is

$$\text{survey rate } (21.3 < R < 22.3) = \frac{N_{SN}}{\sum_i \text{area}_i \times \Delta T_i},$$

where $N_{SN} = 3$ is the number of SNe we found in the 1 mag range and $\Delta T_i$ is the control time for field $i$, computed for an SN with magnitude $R = 21.8$ at maximum. For example, a value of $\Delta T_i = 21$ days was found for the field containing SN 1994H observed on 1993 December 19 and 1994 January 12, i.e., 24 days apart.

We measure a survey rate for $21.3 < R < 22.3$ of $34.4^{+23.9}_{-16.2}$ SNe yr$^{-1}$ deg$^{-2}$ (the error quoted is statistical only). In practice this translates to 1.73 SNe per square degree discovered with a 3 week baseline in data with a limiting magnitude (3 $\sigma$) of $R \sim 23$. The total number of

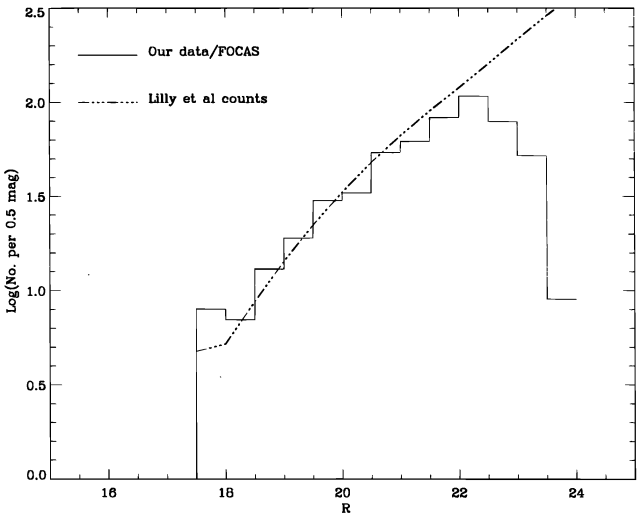


FIG. 2.—Number of galaxies as a function of magnitude determined from one of our noncluster images using FOCAS. The dash-dotted line shows the counts derived from the analysis of Lilly et al. (1995), integrated over the redshift range $0 < z < 2$ and normalized to the image area of 0.03 deg$^2$.

galaxies with $R < 23.8$ surveyed in the 52 fields is approximately 32,000.

## 4. GALAXY COUNTS

In order to compare the distant SN rate with local equivalents, we need to know the redshifts of the galaxies that we have surveyed. We estimate these in a statistical manner by using various groups' analyses of galaxy evolution. In this work, we use the galaxy counts derived from the analysis of Lilly et al. (1995) to estimate the number of galaxies sampled as a function of redshift. We have also carried out the analysis using the galaxy evolution model of Gronwall & Koo (see, e.g., Gronwall & Koo 1995) and that used by Glazebrook et al. (1995), to give an estimate of the sensitivity of our results to the assumed form of galaxy evolution.

$R$-band counts as a function of redshift were calculated by S. Lilly based on the analysis of magnitude-redshift data obtained in the Canada-France Redshift Survey (CFRS; see Lilly et al. 1995 and references therein). The survey contains $\sim$730 galaxies with $17.5 < I < 22.5$. Lilly et al. estimated the expected distribution of galaxies with redshift and $R$-band magnitude, $N(z, R)$, by extrapolation from the $I$-band data, with the implicit assumption that the galaxy population does not evolve at redshifts outside the limits of the CFRS sample. A deceleration parameter $q_0 = 0.5$ was assumed for these calculations (the effect of this assumption on the derived SN rate is discussed in § 6). Since the $I$ band is close to the $R$ band, and the magnitude range of the CFRS sample is comparable to that of our data, this extrapolation is small.

To check that the assumed distribution of galaxies with $R$ magnitude and redshift, $N(z, R)$, yields reasonable galaxy counts compared to our data, we have plotted the number of field galaxies classified by the FOCAS software package, as a function of apparent magnitude, on one of the search

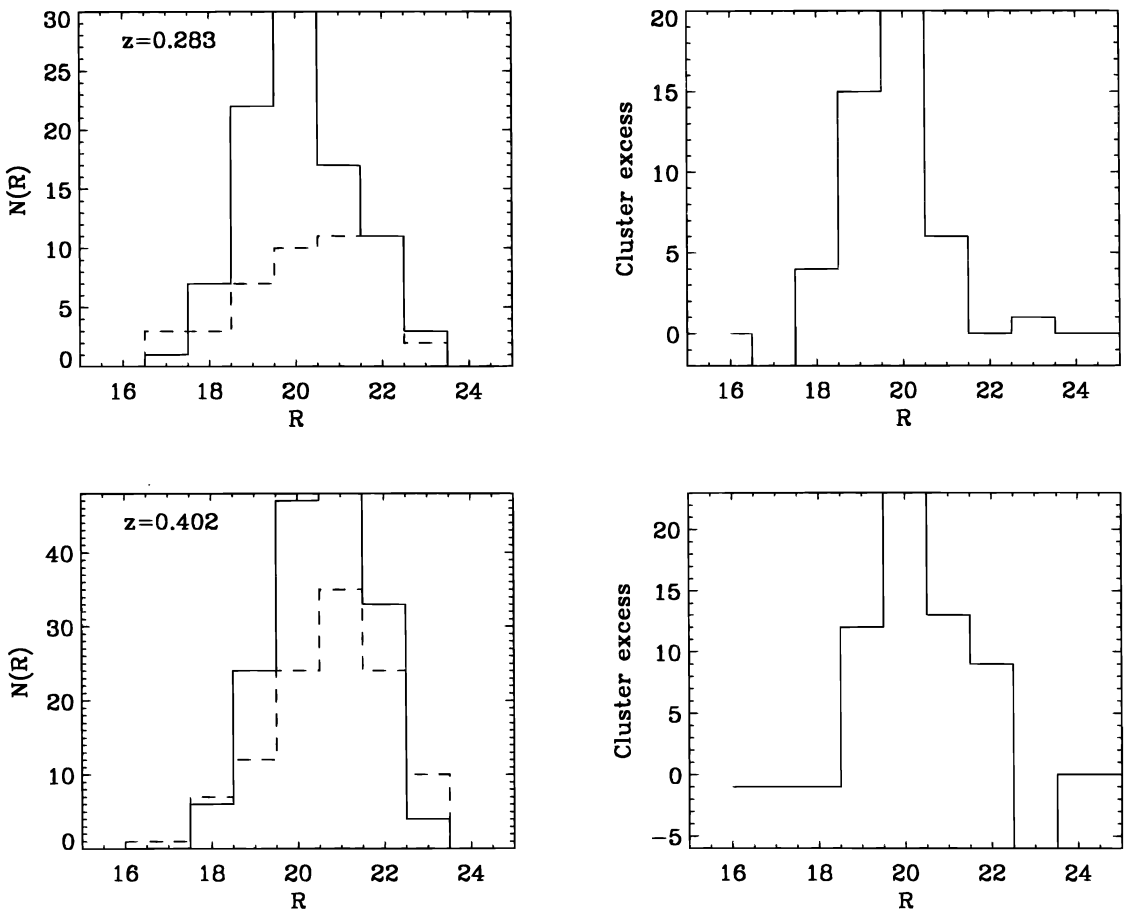


FIG. 3.—Galaxy $N(R)$ in a 500 × 500 pixel box containing the cluster (*solid histograms*) and $N(R)$ in a similar box away from the cluster (*dashed histograms*) for two fields. The excess cluster counts are shown in the right-hand panels.

TABLE 2

TOTAL LUMINOSITY

| | LUMINOSITY ($10^{10} L_{B\odot}$) | | | | | |
|---|---|---|---|---|---|---|
| $R$ | $z = 0.05$ | $z = 0.15$ | $z = 0.25$ | $z = 0.35$ | $z = 0.45$ | $z = 0.55$ |
| 18.5..... | 12.94 | 824.9 | 2808 | 3671 | 881.4 | 88.43 |
| 19.5..... | 7.942 | 322.6 | 2451 | 5368 | 3691 | 2031 |
| 20.5..... | 3.799 | 154.7 | 943.1 | 3520 | 6050 | 6430 |
| 21.5..... | 1.647 | 87.31 | 397.2 | 1281 | 3059 | 6699 |
| 22.5..... | 1.211 | 30.60 | 226.4 | 587.2 | 1243 | 2728 |
| 23.5..... | 1.126 | 11.26 | 88.16 | 340.4 | 744.2 | 1212 |
| 24.5..... | 0.1458 | 18.56 | 17.07 | 105.8 | 351.5 | 799.2 |
| 25.5..... | 0.00 | 9.939 | 60.59 | 27.68 | 65.53 | 280.5 |

NOTES.—Total luminosity given by the counts of Lilly et al. 1995 and assuming $q_0 = 0.5$, in the survey area of 1.73 deg$^2$. Bin widths are 0.1 in $z$ and 1.0 mag in $R$, centered on the values shown.

images that was *not* targeted at a galaxy cluster (Fig. 2). The $R$-band galaxy counts given by the analysis of Lilly et al. (1995), integrated over the redshift range $0 < z < 2$ (*dash-dotted line*), are shown on the same scale, assuming an effective area for this image of 0.03 deg$^2$.

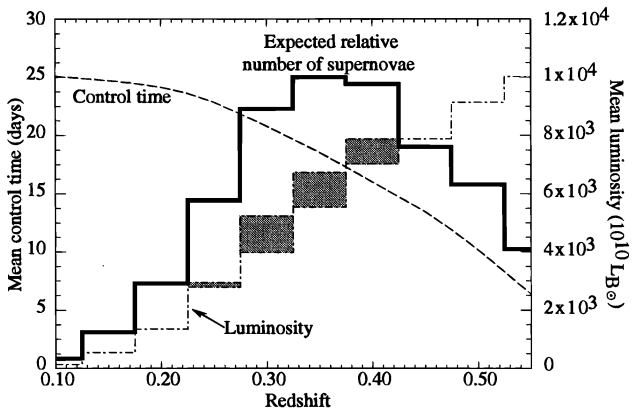


FIG. 4.—Expected number of supernovae as a function of $z$ (*solid histogram*) together with the overall detection efficiency given as a "control time" (*dashed line*) and the luminosity-weighted number of galaxies (*dash-dotted histogram*). The contribution to the luminosity from clusters is shown by the shaded area. The 1993 December–1994 January search was most likely to find SNe with redshifts between $z = 0.3$ and $z = 0.4$. Between $z = 0.3$ and $z = 0.55$, the search was more than 50% efficient. Note that our more recent searches go deeper than this data.

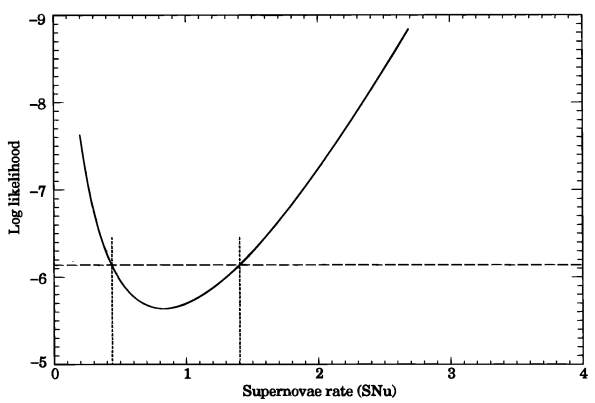


FIG. 5.—Results from the maximum likelihood fit of the observed distribution of SN events to the expected distribution, $N_{exp}(z)$. The dashed vertical lines show the $\pm 1\,\sigma$ uncertainty in the result.

Many of our search fields were chosen specifically to target high-redshift clusters. For each of these fields, we estimate the number of cluster galaxies by counting galaxies as a function of $R$ magnitude in a box of size 500 × 500 pixels centered approximately on the center of the cluster, as estimated by eye from the images. The counts in a similar box in a region of the image away from the cluster were subtracted from the cluster counts to obtain the cluster excess counts as a function of $R$ magnitude. Examples of these distributions are shown in Figure 3. Typically a cluster contributes 10% of the galaxy counts on an image. We assign these galaxies to the cluster redshift, and add the cluster contribution to the $N(z, R)$ for that image given by the models.

## 5. TYPE Ia SUPERNOVA RATES

To compare our derived SN rate with local rates, we express the rate in units of SNu, the number of SNe per century per $10^{10}$ solar luminosities in the rest-frame $B$ band. To calculate the rate, we derive the expected redshift distribution of SNe, $N_{exp}(z)$, which is proportional to the observed SN rate, $r_{SN}(1+z)^{-1}$, where $r_{SN}$ is the rate in the rest frame of the supernovae. The expected distribution is

$$N_{exp}(z) = \frac{r_{SN}}{1+z} \sum_R \sum_i N_{gal}(z, R)_i L_B(z, R) \Delta T_i(z, R) ,$$

where $i$ runs over all fields, $R$ is the galaxy apparent $R$ magnitude, and $L_B$ is the galaxy rest-frame $B$-band luminosity in units of $10^{10} L_{B\odot}$. We then fit the observed redshift distribution to $N_{exp}$ and hence derive $r_{SN}$. Here it is assumed that the rest-frame rate $r_{SN}$ is constant in the redshift range of interest ($0.3 \lesssim z \lesssim 0.5$). The control times $\Delta T$, in units of centuries, have been calculated for each field in bins of $z$ and $R$ (the size of the bins used is 0.5 mag in $R$ and 0.05 in $z$). The derived rate corresponds to a mean redshift of

$$\langle z \rangle = \int z N_{exp}(z) dz \Big/ \int N_{exp}(z) dz .$$

To compute the rest-frame $B$-band galaxy luminosities from apparent $R$ magnitudes, we used $B - R$ colors and $B$-band $K$-corrections (which include the effects of evolution) supplied by C. Gronwall and D. Koo (1995, private communication). These are based on the models of Gronwall & Koo (1995), which give the relative proportions in each bin of $z$ and apparent $R$ magnitude of three different color classes of galaxies (defined as "red," $B-V > 0.85$; "green," $0.6 < B-V < 0.85$; and "blue," $B-V < 0.6$). Note that the combined color, $K$-, and evolution correction is small in the redshift range of interest (0.3–0.5), mostly because the observed $R$ band is close to the rest-frame $B$ band.

The appropriate correction for each color class was applied in the proportions given by the model, and the total luminosity of galaxies in that bin was computed. In this calculation, $M_{B\odot} = 5.48$ and $q_0 = 0.5$ were assumed. Table 2 lists the total luminosity in bins of $z$ and $R$ magnitude.

Figure 4 shows the expected redshift distribution of SNe, $N_{exp}(z)$, as calculated above. The detection efficiency as a function of $z$, expressed as the mean control time $\Delta T$, averaged over all fields is also shown, as well as the mean galaxy counts weighted by their $B$-band luminosities. These two mean quantities are shown merely for illustration; they are

not used in the calculation of the expected distribution, since each field is treated separately and the results combined.

The rest-frame supernovae rate, $r_{SN}$, at $z \sim 0.4$ was obtained by fitting the redshift distribution of observed SNe to the expected distribution $N_{exp}(z)$ by using a maximum likelihood fit with Poisson statistics (Fig. 5). The mean redshift corresponding to this rate is $\langle z \rangle = 0.38$. We derive a value for the SN rate of

$$r_{SN}(z = 0.38) = 0.82^{+0.54}_{-0.37} h^2 \text{ SNu} ,$$

where the error is statistical only.

## 6. SYSTEMATIC UNCERTAINTIES

Because of the small number of SNe in this first sample, the total uncertainty in this measurement is dominated by statistics. We have nevertheless estimated the following systematic uncertainties. The sources studied are listed below, and Table 3 summarizes their contributions.

*Total luminosity estimate.*—The total solar luminosity to which the survey is sensitive was estimated by using counts for $N(z, R)$, which have statistical uncertainty due to the finite number of galaxies used in the analysis (e.g., $\sim 700$ in the analysis of Lilly et al. 1995). The statistical uncertainty in the model contributes about $\pm 0.02\ h^2$ SNu uncertainty to the rate.

In addition, the luminosity estimation depends on the deceleration parameter since $q_0$ enters into the galaxy $N(z, R)$ model/predicted counts, the $K$-corrections of Gronwall & Koo (1995), and the luminosity distance used to calculate the galaxy absolute luminosities. To estimate the sensitivity of our result to $q_0$, we repeated the analysis using versions of the Lilly et al. counts and the Gronwall & Koo model that were calculated for $q_0 = 0.0$. This value of $q_0$ was also used to calculate the luminosity distances. The deceleration parameter does not affect the calculation of control times, because the observed light curves are used in this calculation. The total effect is small and is dominated by the effect on the luminosity distance. Using $q_0 = 0.0$ rather than 0.5 lowers the derived rate by $0.08\ h^2$ SNu. Similarly, increasing $q_0$ by 0.5 raises the rate by a comparable amount.

The combined uncertainty in the rate due to the luminosity estimate is therefore $\pm 0.09\ h^2$ SNu.

TABLE 3

SYSTEMATIC UNCERTAINTIES

| Source | Uncertainty ($h^2$ SNu) |
|---|---|
| Luminosity estimate | 0.09 |
| Cluster contribution | 0.02 |
| Galactic extinction | 0.01 |
| APM calibration | 0.10 |
| Detection efficiency | 0.08 |
| Range of Ia light curves | 0.19 |
| Scanning efficiency | $^{+0.27}_{-0.00}$ |
| Total | $^{+0.37}_{-0.25}$ |

NOTES.—All uncertainties were estimated using the Lilly et al. 1995 counts for the magnitude-redshift distribution of galaxies, $N(R, z)$. Note that no estimate of systematic uncertainties from galaxy counts or from galaxy inclination and extinction was made.

*Contribution from clusters.*—Many of our fields contain a known cluster in the redshift range $z = 0.3$–$0.5$. Four of our fields contain visible clusters that do not have known redshifts. To estimate the effect this uncertainty has on the derived rate, we assigned all the unknown redshifts to $z = 0.1$ and in separate analyses assigned their redshifts to $z = 0.7$ and $z = 0.4$, where this search is most sensitive. The effect of changing the assumed $z$ from 0.1 to 0.4 is to decrease the rate by $0.01\ h^2$ SNu. Similarly, changing the assumed redshifts from $z = 0.4$ to $z = 0.7$ lowers the rate by $0.01\ h^2$ SNu. There is also some uncertainty due to the faint cluster galaxies that are not detected on our images, but which could host a detectable SN. We estimate less than a 10% uncertainty in calculating the overall contribution to the galaxy counts from these clusters, yielding a contribution of $\pm 0.02\ h^2$ SNu to the uncertainty in the SN rate.

*Extinction correction.*—The uncertainty from correcting for extinction was calculated by following the estimate from Burstein & Heiles (1982) of the uncertainties in deriving the Galactic reddening. The effect on the rate is small, amounting to $\pm 0.01\ h^2$ SNu.

*APM calibration.*—Although we used measured SN light curves, calibrated with Landolt standards, to calculate the control times, the galaxies were calibrated by use of the less accurate APM calibration. Errors in the APM calibration of the fields would thus alter the determination of the efficiency as a function of magnitude. This has a sizable effect on the derived SN rate since, at the magnitude of most of our SNe, the detection efficiency varies rapidly with magnitude. We estimated the size of the effect by using the current best estimate of $\pm 0.2$ mag uncertainty in the APM calibration of our fields; this contributes $\pm 0.10\ h^2$ SNu to the rate uncertainty (in the sense that brighter assigned magnitudes reduce the derived rate).

*Efficiency determination.*—Detection efficiencies were determined by using a Monte Carlo simulation that was statistically limited (100 fake SNe were added to each image). In addition, models were used for the distance of the SN to the host and the host galaxy magnitude distribution (assumed to be representative of the total galaxy population). Figure 1*d* shows, however, that the detection efficiency depends only weakly upon the magnitude difference between the host galaxy and the SN and, therefore, upon the position of the SN on the host and the host-magnitude distribution. We estimated less than 5% uncertainty on the efficiency from using these assumptions. Altogether, uncertainties in the calculation of the efficiency amount to $\pm 0.08\ h^2$ SNu uncertainty in the rate.

*Range of Type Ia SN light curves.*—Control times were calculated using a single-template light curve with a peak brightness calibrated using the mean of the three observed SNe, therefore making the assumption that Type Ia SNe are standard candles. However, the observed rms scatter in peak brightness for Type Ia SNe could be as large as 0.5 mag, depending on the sample used (Riess, Press, & Kirshner 1995; Vaughan et al. 1996). A correlation between peak brightness and light-curve width (Phillips 1993; Hamuy et al. 1995; Riess et al. 1995) can nevertheless be used to reduce the scatter to 0.21 mag or better (Hamuy et al. 1995; Riess et al. 1995). We therefore estimate a 1 $\sigma$ systematic effect on the measured rate, assuming that the overall scatter in brightness of 0.5 comes from two independent sources: (1) An "intrinsic" scatter of 0.21 mag, independent of light-curve width. This was estimated by altering the

peak magnitude of the template light curve by $0.21/(\sqrt{3}$ mag, which had the effect of changing the rate by 0.07 $h^2$ SNu. (2) A contribution of 0.45 $[=(0.5^2-0.21^2)^{1/2}]$ mag correlated with light-curve width. This was estimated by altering the peak brightness by $0.45/\sqrt{3}$ mag and, correspondingly, the width of the template light curve. To do this we used an approximation for the width-magnitude relation, following the "stretch factor" method of Perlmutter et al. (1996a), which reproduces the results of Hamuy et al. (1995) and Riess et al. (1995). This changes the rate by 0.18 $h^2$ SNu. The overall uncertainty due to the intrinsic and calibratable dispersion of Type Ia light curves therefore amounts to $\pm 0.19$ $h^2$ SNu on the rate. Note that this is a conservative estimate since magnitude-limited samples yield observed dispersions in peak magnitude of $\sim 0.35$ mag, as compared to $\sim 0.5$ mag for volume-limited samples.

*Scanning efficiency.*—One SN candidate, the faintest, was not followed up (see § 2). If this was indeed a Type Ia event, then the estimate of the rate increases by 0.27 $h^2$ SNu.

For any assumed galaxy counts, the main contribution to the systematic uncertainty comes from the range of Type Ia SN light curves. High-redshift supernovae from ongoing searches, including the recent 11 discoveries of this group, will soon bring down the statistical uncertainty so that the systematic uncertainty will limit the accuracy of high-redshift SN rate measurements. The sensitivity to the assumed galaxy counts was not included in this estimation and is discussed in the next section. Assuming the Lilly et al. counts for $N(z, R)$, we estimate the total systematic error to be $^{+0.37}_{-0.25}$.

## 7. DISCUSSION

*Galaxy counts.*—To test the sensitivity of our result to the galaxy counts, we recalculated the rate using the model of Gronwall & Koo (1995) and that used by Glazebrook et al. (1995).

The galaxy counts of Gronwall & Koo were kindly provided by C. Gronwall, and are based on the analysis in Gronwall & Koo (1995). The model is a "passive evolution" model that has been constrained using galaxy counts in various bands, principally $B_J$, and color and redshift distributions for various ranges of $B_J$ (see Koo, Gronwall, & Bruzual 1993). In determining their model from the data, $H_0 = 50$ km s$^{-1}$ Mpc$^{-1}$ and $q_0 = 0.5$ were assumed. A nonstandard local luminosity function is assumed to minimize evolution, required to fit the counts.

The model used by Glazebrook et al. (1995) was also used. This model was derived by using the local luminosity function of Loveday et al. (1992), the morphological mix given by Shanks et al. (1984), and $K$-corrections based on spectral templates of Rocca-Volmerange & Guiderdoni (1988). In determining the model, $q_0 = 0.5$ was assumed. A normalization $\phi^* = 0.03[1\ h/(1\ \mathrm{Mpc})]^3$ was used in this analysis.

These models are quite different, as can be seen in Figure 6, where a comparison of the $R$-magnitude distribution between Lilly et al. counts and the counts derived from Gronwall & Koo and Glazebrook et al. models shows very substantial differences in the redshift range $0.2 < z < 0.6$, where our SN search is most sensitive. The rate that we derive by using the model of Gronwall & Koo is $1.61^{+1.05}_{-0.73}$ $h^2$ SNu, almost a factor of 2 higher than the value derived by using the Lilly et al. counts. Using Glazebrook et al.'s model, we derive a value for the rate of $1.27^{+0.83}_{-0.57}$ $h^2$ SNu,

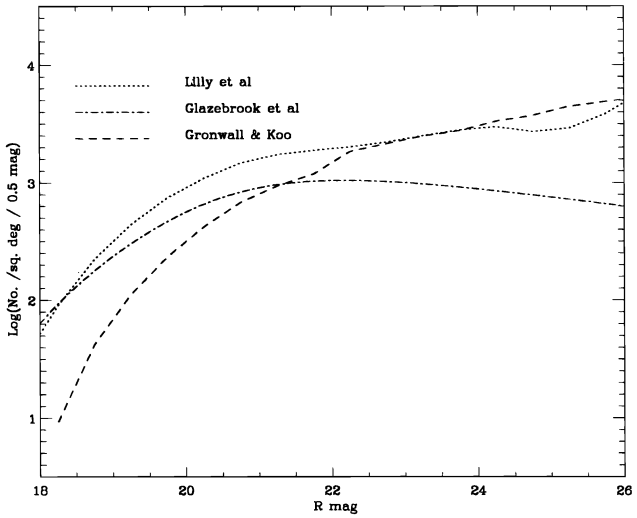


FIG. 6.—Comparison of the galaxy $N(R)$ in the redshift range $0.2 < z < 0.6$. The counts of Lilly et al. (derived from the analysis of Lilly et al. 1995), and the models of Gronwall & Koo (1995) and Glazebrook et al. (1995) are shown. The fluctuations in the curves reflect the statistical fluctuations in the data from which the models were derived.

which differs by 50% from the rate derived using the Lilly et al. counts.

Before drawing any conclusion from these results, it should be noted that, unlike the galaxy counts derived from the above models, Lilly et al. counts are based on data that are well matched to our survey in magnitude and redshift range, and only small amount of extrapolation was required in converting from the $I$ to the $R$ band. We therefore believe that the large differences between the results reflects uncertainties in the extrapolation of the models of Gronwall & Koo and Glazebrook et al. to match our data set, and we do not quote any systematic uncertainty from galaxy counts in Table 3.

*Host galaxy inclination and extinction.*—The effect of host galaxy inclination on detection efficiency and host galaxy luminosity estimates should be taken into account when calculating supernova rates. Cappellaro et al. (1993b) and van den Bergh & Tammann (1991) have estimated the inclination correction factors for nearby searches. In this analysis, both the search technique (in our case, subtraction of CCD images) and calculation of the galaxies' luminosities were done differently than in most nearby searches, and the effects of galaxy inclination should not be the same.

Galaxy inclination and extinction would reduce both the number of supernovae detected and the galaxy visible luminosity. These effects may therefore partially cancel in the calculation of the rate. A complete analysis of this effect would require modeling of galaxy opacities, which is beyond the scope of this paper. We therefore compare our uncorrected value with uncorrected values for nearby searches, with particular attention to CCD searches.

*Consistency check.*—This analysis is based on a subsample of data taken during winter 1994. The larger sample of seven SNe was discovered in approximately double this number of fields in three different periods of data taking. Preliminary analysis of this data shows consistency with the results presented here. As a further consistency check, we have examined the original data set for SNe that are past maximum light. This was done by subtracting the search

images from the reference images (the reverse of the usual method) and searching for positive signal as before. Two possible SNe were found in this way, consistent with the number discovered on the rise. Since we have no further information on whether these are Type Ia SNe, they have not been included in our determination of the rate.

*Detection efficiencies.*—The study of detection efficiencies as a function of SN magnitude is a key element of this analysis. These efficiencies depend upon many parameters and vary widely from field to field. It is therefore essential to carefully and systematically estimate them. The knowledge of these efficiencies will also be very useful for estimating the effects of Malmquist bias on our sample of SNe. This will be particularly important when using the distribution of measured peak magnitudes to estimate $q_0$. At $z \sim 0.4$, the present mean efficiency curve, applied to a Gaussian distribution of peak magnitude with 0.2 mag intrinsic dispersion, would lead to a shift in the derived value of $q_0$ of $\sim 0.1$ if not taken into account.

*Comparison with other measurements.*—This is the first direct measurement of the Type Ia rate at high redshift. In their pioneering work, searching for high-redshift supernovae, Hansen et al. (1989) discovered a probable Type II event at $z = 0.28$ and a Type Ia event at $z = 0.31$ (Nørgaard-Nielsen et al. 1989). No estimates of SN rates were published after the Type Ia discovery, but beforehand they had concluded that their observation was in mild disagreement with an expected number of Type Ia's (based on local rates) of 2.2–9.2 (the range indicates the range of determinations of the local rate from van den Bergh, McClure, & Evans 1987 and Cappellaro & Turatto 1988).

Nearby supernovae rates have recently been carefully reanalyzed (Cappellaro et al. 1993a, 1993b; Turatto, Cappellaro, & Benetti 1994; van den Bergh & McClure 1994; Muller et al. 1992), using more precise methods for calculating the control times and correcting for inclination and overexposure of the nuclear regions of galaxies in photographic searches. The rates obtained for Type Ia SNe are now consistent among these groups and vary between 0.2 and 0.7 $h^2$ SNu, depending on the galaxy types (E, Sa, etc.; higher rates are found in later-type galaxies).

In order to compare these rates with our measurements, one should remember that (1) most local measurements have been based on photographic data rather than CCD data as used here, (2) we did not apply any correction for host galaxy absorption and inclination, and (3) at $z \sim 0.4$ the ratios of galaxy type are different. Using galaxy counts from Gronwall & Koo in the range $0.35 < z < 0.45$ and $21.75 < R < 22.25$ and their color classification of galaxies (C. Gronwall 1995, private communication), we estimate the relative fraction of galaxy types in our sample to be 23% E–S0, 15% S0a–Sb, and 62% Sbc–Sd. Combining this with the Type Ia rates measured by Cappellaro et al. (1993b) for E–S0, S0a–Sb, and Sbc–Sd galaxy types, we can calculate the local rate that we should find if the mix of galaxies locally is the same as the mix at $z \sim 0.4$. We obtain $0.53 \pm 0.25$ $h^2$ SNu. Our measured value of $0.82^{+0.65}_{-0.45}$ $h^2$ SNu (where statistical and systematic uncertainties have been combined), although slightly higher, agrees with this value within the uncertainty and indicates that Type Ia rates do not change dramatically out to $z \sim 0.4$. Note, however, that correcting for host galaxy extinction and inclination may change this conclusion.

Theoretical estimates of Type Ia SN rates have been derived from stellar and galaxy evolution models. Calculations were performed mostly for elliptical galaxy types. Earlier calculations predicted lower than observed rates for Type Ia's (Tornambè & Matteucci 1986, 1987; Tornambè 1989). More recent calculations, based on evolutionary models of elliptical galaxies, predict rates of $\sim 0.1$ $h^2$ SNu (Ferrini & Poggianti 1993). Assuming a factor of $\sim 2$ higher rate in nonelliptical galaxies compared to ellipticals (Cappellaro et al. 1993b) and a mix of galaxy types as above, we convert this to an overall rate of Type Ia SNe at $z \sim 0.4$ in all galaxy types and derive a value of $\sim 0.37$ $h^2$ SNu. Our total uncertainty of $^{+0.65}_{-0.45}$ in the measurement presented in this paper does not allow any firm conclusion, but our observed rate seems to lie above this theoretical prediction. There may be an increase of Type Ia rate with redshift. Ruiz-Lapuente et al. (1995) predicted a significant increase in rate for redshifts between 0.4 and 0.8, depending on the specific model they considered. In the near future, our ongoing high-$z$ SN search and others should provide enough data to constrain the theoretical calculations.

This work was supported in part by the National Science Foundation (ADT 88-909616) and the US Department of Energy (DE-AC03-76SF000098). We thank the La Palma staff and observers for carrying out service observations. We also thank Simon Lilly and Caryl Gronwall and David Koo for providing their galaxy counts prior to publication, and Richard Kron for useful discussions. I. M. H. acknowledges a NATO fellowship. R. P. thanks Gerard Fontaine of CNRS-IN2P3 and Bernard Sadoulet of the Center for Particle Astrophysics, Berkeley, for supporting his participation in this project.

## REFERENCES

Burstein, D., & Heiles, C. 1982, AJ, 87, 1165
Cardelli, J. A., Clayton, G. C., & Mathis, J. S. 1989, ApJ, 345, 245
Cappellaro, E., & Turatto, M. 1988, A&A, 190, 10
Cappellaro, E., Turatto, M., Benetti, S., Tsvetkov, D. Yu., Bartunov, O. S., & Makarova, I. J. 1993a, A&A, 268, 472
———. 1993b, A&A, 273, 383
Ferrini, F., & Poggianti, B. 1993, ApJ, 410, 44
Glazebrook, K., Ellis, R., Santiago, B., & Griffiths, R. 1995, MNRAS, 275, L19
Gronwall, C., & Koo, D. 1995, ApJ, 440, L1
Gunn, J. E., Hoessel, J. G., & Oke, J. B. 1986, ApJ, 306, 30
Hamuy, M., Phillips, M. M., Maza, J., Suntzeff, N. B., Schommer, R., & Avilés, R. 1995, AJ, 109, 1
Hansen, L., Jørgensen, H. E., Nørgaard-Nielsen, H. U., Ellis, R. S., & Couch, W. J. 1989, A&A, 211, L9
Kim, A., Goobar, A., & Perlmutter, S. 1996, PASP, 108, 190
Koo, D., Gronwall, C., & Bruzual A., G. 1993, ApJ, 415, L21
Landolt, A. U. 1992, AJ, 104, 340
Leibundgut, B. 1988, Ph.D. thesis, Univ. Basel
Lilly, S., Tresse, L., Hammer, F., Crampton, D., & Le Fèvre, O. 1995, ApJ, 455, 108
Loveday, J., Peterson, B. A., Efstathiou, G., & Maddox, S. J. 1992, ApJ, 400, L43
McMahon, R. G., & Irwin, M. J. 1992, in Digitised Optical Sky Surveys, ed. H. T. MacGillivray & E. B. Thomson (Dordrecht: Kluwer), 417
Muller, R. A., Newberg, H. J. M., Pennypacker, C. R., Perlmutter, S., Sasseen, T. P., & Smith, C. K. 1992, ApJ, 384, L9
Nørgaard-Nielsen, H. U., Hansen, L., Jørgensen, H. E., Aragón-Salamanca, A., Ellis, R. S., & Couch, W. J. 1989, Nature, 339, 523
Perlmutter, S., et al. 1996a, in Thermonuclear Supernovae, ed. R. Canal, P. Ruiz-Lapuente, & J. Isern (NATO ASI Ser. C) (Dordrecht: Kluwer), in press
———. 1995a, IAU Circ. 6270
———. 1995b, ApJ, 440, L41
———. 1994, IAU Circ. 5956
———. 1995c, IAU Circ. 6263
———. 1996b, in preparation
Phillips, M. M. 1993, ApJ, 413, L105

Riess, A. G., Press, W. H., & Kirshner, R. P. 1995, ApJ, 438, L17
Rocca-Volmerange, B., & Guiderdoni, B. 1988, A&AS, 75, 93
Ruiz-Lapuente, P., Burket, A., & Canal, R. 1995, ApJ, 447, L69
Shanks, T. S., Stevenson, P. R., Fong, R., & MacGillivray, H. T. 1984, MNRAS, 206, 767
Tornambè, A. 1989, MNRAS, 239, 771
Tornambè, A., & Matteucci, F. 1986, MNRAS, 223, 69
———. 1987, ApJ, 318, L25
Turatto, M., Cappellaro, E., & Benetti, S. 1994, AJ, 108, 202
van den Bergh, S., & McClure, R. D. 1994, ApJ, 425, 205
van den Bergh, S., McClure, R. D., & Evans, R. 1987, ApJ, 323, 44
van den Bergh, S., & Tammann, G. A. 1991, ARA&A, 29, 363
Vaughan, T. E., Branch, D., & Perlmutter, S. 1996, in preparation